Supplemental Material:

Negative differential resistance state in the free - flux - flow regime of driven vortices in a single crystal of $2H$ -NbS_2

Biplab Bag[1,+], Sourav M. Karan[1], Gorky Shaw[2], A. K. Sood[3], A. K. Grover[4] & S. S. Banerjee[1,*]

[1] Department of Physics, Indian Institute of Technology, Kanpur, 208016, India
[2] National Physical Laboratory, Hampton Road, Teddington TW11 0LW, United Kingdom
[3]Department of Physics, Indian Institute of Science, Bengaluru, 560012, India
[4]Department of Applied Sciences, Punjab Engineering College, Chandigarh 160012, India
[+]Present Address: DCMPMS, Tata Institute of Fundamental Research, Mumbai, 400005, India
*email: satyajit@iitk.ac.in

1. **<u>NDR seen in a sample from a different batch (Another Sample from different batch (A2 batch of Ref. 27, B. Bag, et al., Sci. Rep. 7, 5531 (2017)))</u>**

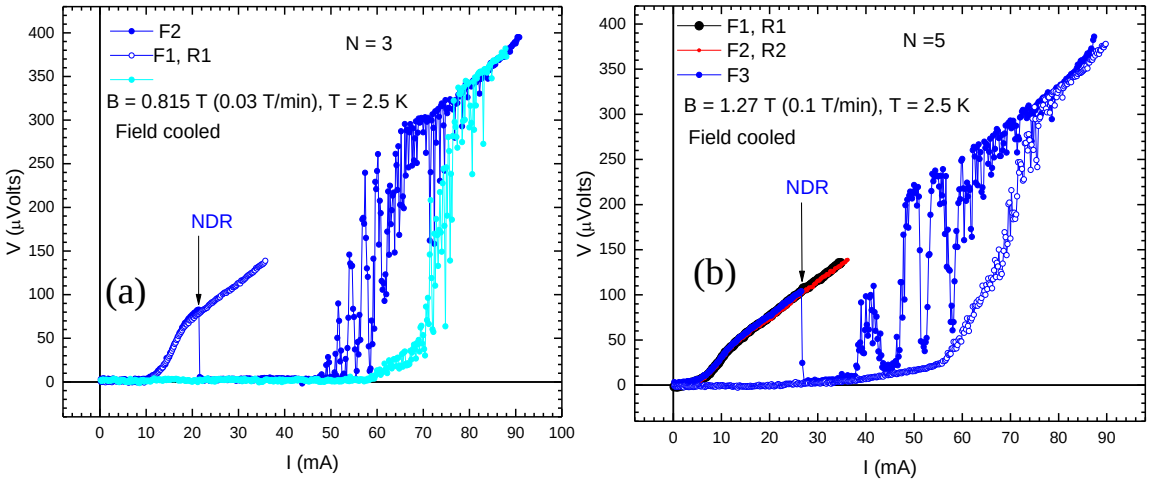

Figure S1: (a) shows onset of NDR after two cycling at 0.815 T (0.03 T/min) at 2.5 K, FC state. (b) shows onset of NDR after 4 cycling at 1.27 T (0.1 T/min) at 2.5 K, FC state.

From Fig. S1, we see that in this sample (say A2), at 0.815 T and 1.27 T, NDR transition occurs for $N = 3$ and $N = 5$ respectively. Whereas for the sample (say A1) in the present manuscript, in this field regime, $N = 4$. Hence, A2 sample takes one more/less cycle than that in A1. We would like to state that while there maybe slight differences in the absolute value of N from sample to sample, the overall nature of the phenomenon remains unchanged.

2. Structure and composition information

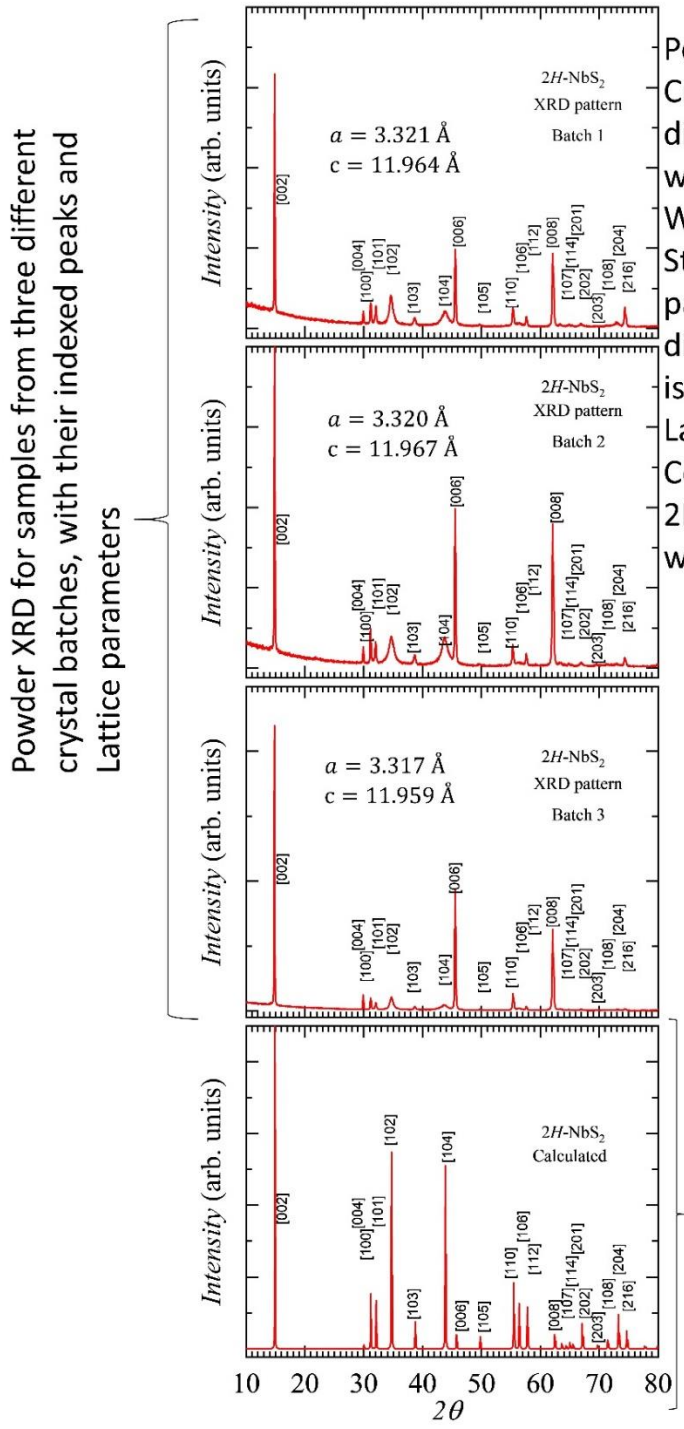

Powder XRD Analysis of Crystals taken from different batches along with their Indexing. We note that the crystalline Structure / lattice parameters, across the different crystal batches is almost uniform. The Lattice parameters Correspond with the 2H phase of NbS2 and we find no 3R phase.

Expected (calculated) peak locations for 2H-NbS_2. The actual Peaks closely match with the expected peak Locations.

EDX: Atomic percentage in 2*H*-NbS_2 samples

Atomic percentage in 2*H*-NbS_2 samples

Batch	Nb (%)	S (%)
1	34.18	65.82
2	34.78	65.22
3	34.63	65.37

EDX analysis was done at different locations on samples from three different batches. The average values are shown in above table. From the analysis, we see that on the average, the atomic ratio, S:Nb > 1.85. This is expected for the 2*H*-NbS_2 compound. The presence of a 3R phase would lead to a much lower S concentration (S:Nb < 1.8). The major components detected by EDX were Nb and S. Other than Nb and S the EBX software showed few other trace elements. The accuracy of the percentages of the minor quantity of other trace elements suggested by the EDX software, isn't certain. As their contributions was less than 0.05% hence we include them within the error bars of 0.05% the above values.

A common issue associated with 2*H*-NbS_2 is that if the growth conditions aren't carefully controlled, then it leads to the formation of the metal rich 3R phase, which is non-superconducting. The presence of a 3R phase in 2*H*-NbS_2 would act as a strong pinning center in the crystal. We show via powder XRD analysis that the lattice parameters as well as the location of the XRD peaks suggest the presence of only 2*H* phase and there is no evidence of the 3R phase in our crystals. The energy dispersive X-ray analysis (EDX) analysis also shows the absence of any 3R phase in the crystals.

3. ***T*-dependence of I_c^h & I_c^l; and demonstration of recovering back low I_c^lstate via field cooling the sample**

For comparison, in Figs. S2(a),(b), we present the *T*-dependence of critical currents for the sample on which data is presented in the main manuscript. We find that I_c^h is *T*-independent while in the same *T* range I_c^l exhibits conventional decrease with increasing *T*. This shows the behaviour of $I_c^h$and I_c^l is quite distinct. Once one enters the I_c^h state, we find that we can recover back the I_c^l state only via going above T_c and then field cooling down and measuring the *I*-*V* at the desired *B*, as shown in the next figure S3.

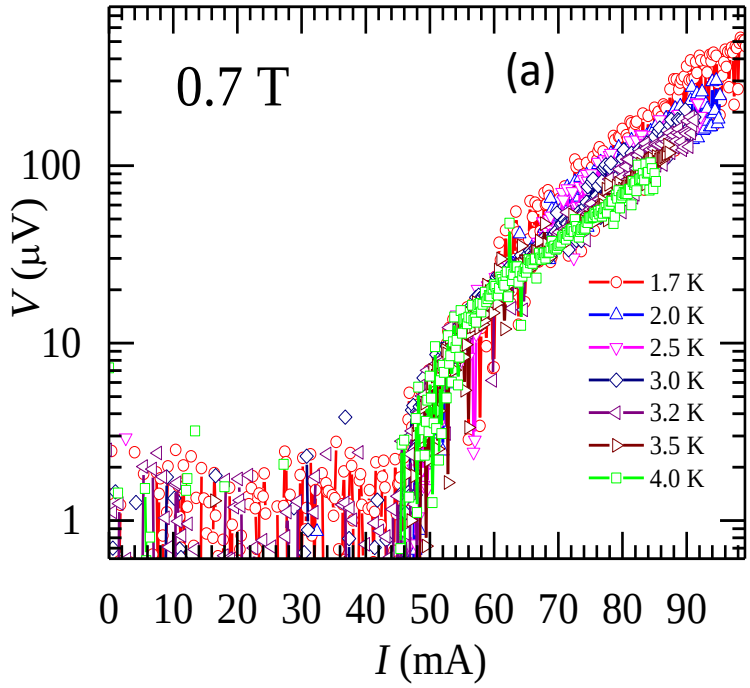

Figure S2 (a): *I*-*V* data at various *T*'s showing depinning curves across I_c^h

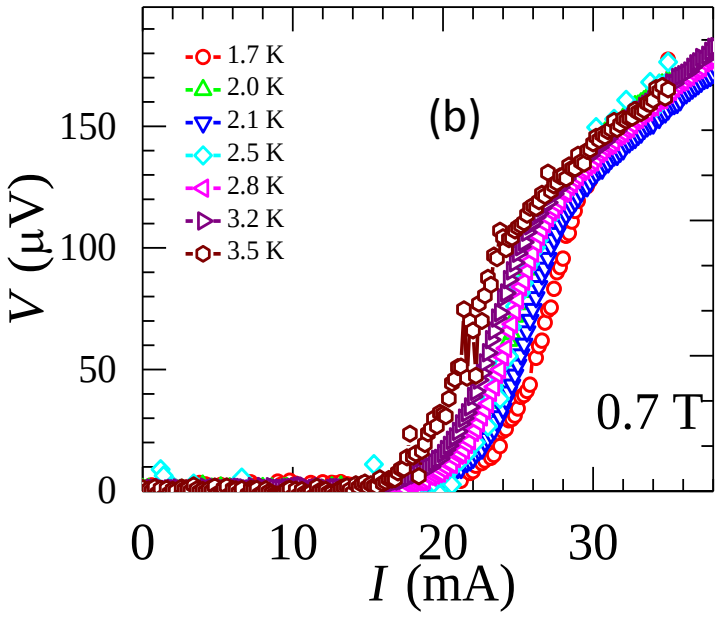

Figure S2 (b): *I*-*V* data at various *T*'s showing depinning curves across I_c^l

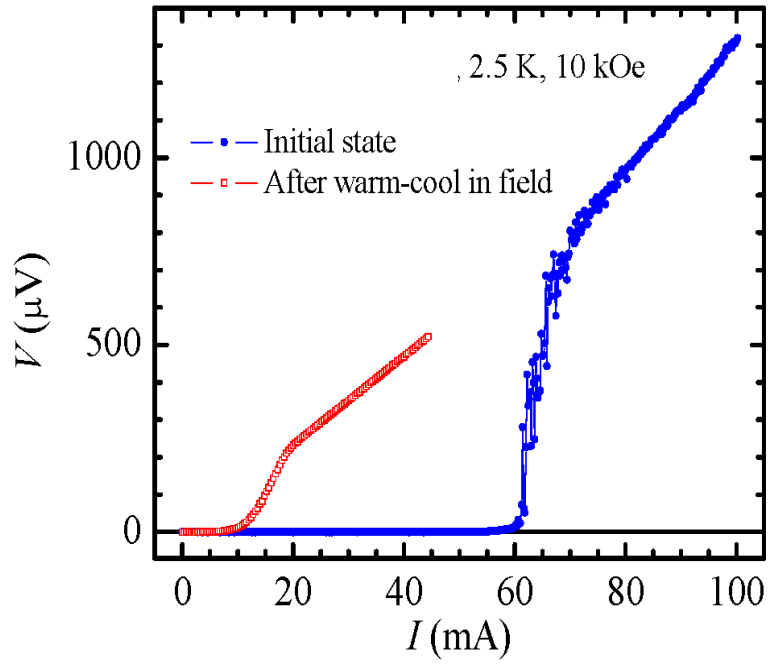

Figure S3: *I-V* response at 2.5 K and 10 kOe of a 2*H*-NbS_2 sample of different batch. The initial state belongs to a zero field cooled vortex state and the after warm-cool state in field corresponds to a field cooled (FC) state

The *I-V* data shown in Fig S3 is measured in the crystal from as different batch of 2*H*-NbS_2 sample. The curve marked as "Initial state", shows the *I-V* corresponding to the high I_c^h ~ 60 mA state attained by *I-V* cycling. Next, without changing the applied magnetic field, we switch off the applied current and warm the sample to 20 K which is well above its T_c (5.8 K), and then cool down to 2.5 K in the applied field of 10 kOe (field cooling). In this field cooled (FC) state, as we measure the *I-V* of the sample, we observe that for this FC state, the driven vortex matter depins from the low I_c^l state. Had regions of structural and/or chemical inhomogeneous regions which act as strong pinning centers which could be responsible for the high I_c state, then upon field cooling we should have obtained the high I_c state rather than the low I_c state, as vortices should have been preferentially pinned on these strong pinning centers.

4. *I-V* response for the jammed high I_c state, reached in *R*(*B*) in Fig. 2 (manuscript)

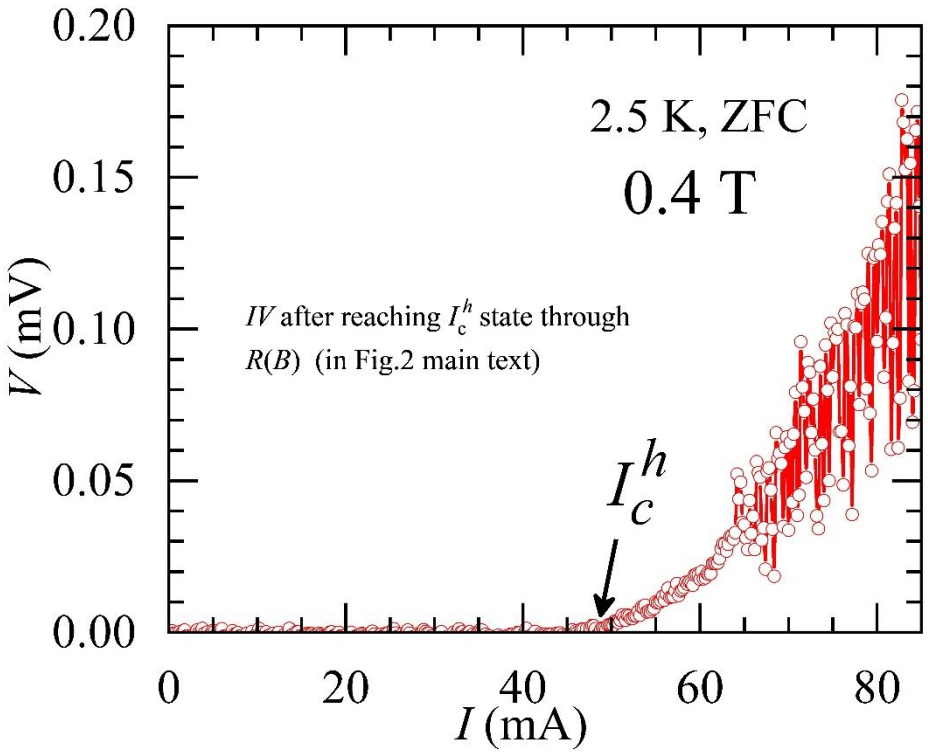

Figure S4: *I-V* response at 2.5 K and 0.4 T (ZFC) for the high I_c state reached via *R*(*B*) in Figure 2 (manuscript)

After transformation from the low to high I_c state, reached in *R*(*B*) measurements (Fig. 2 of manuscript), we measure the *I-V* in that high I_c vortex state (Fig. S4), which exhibits depinning at $I_c^h \sim$ 45 mA.

5. All *I-V* curves associated with Fig. 5 of the manuscript for ZFC and FC states

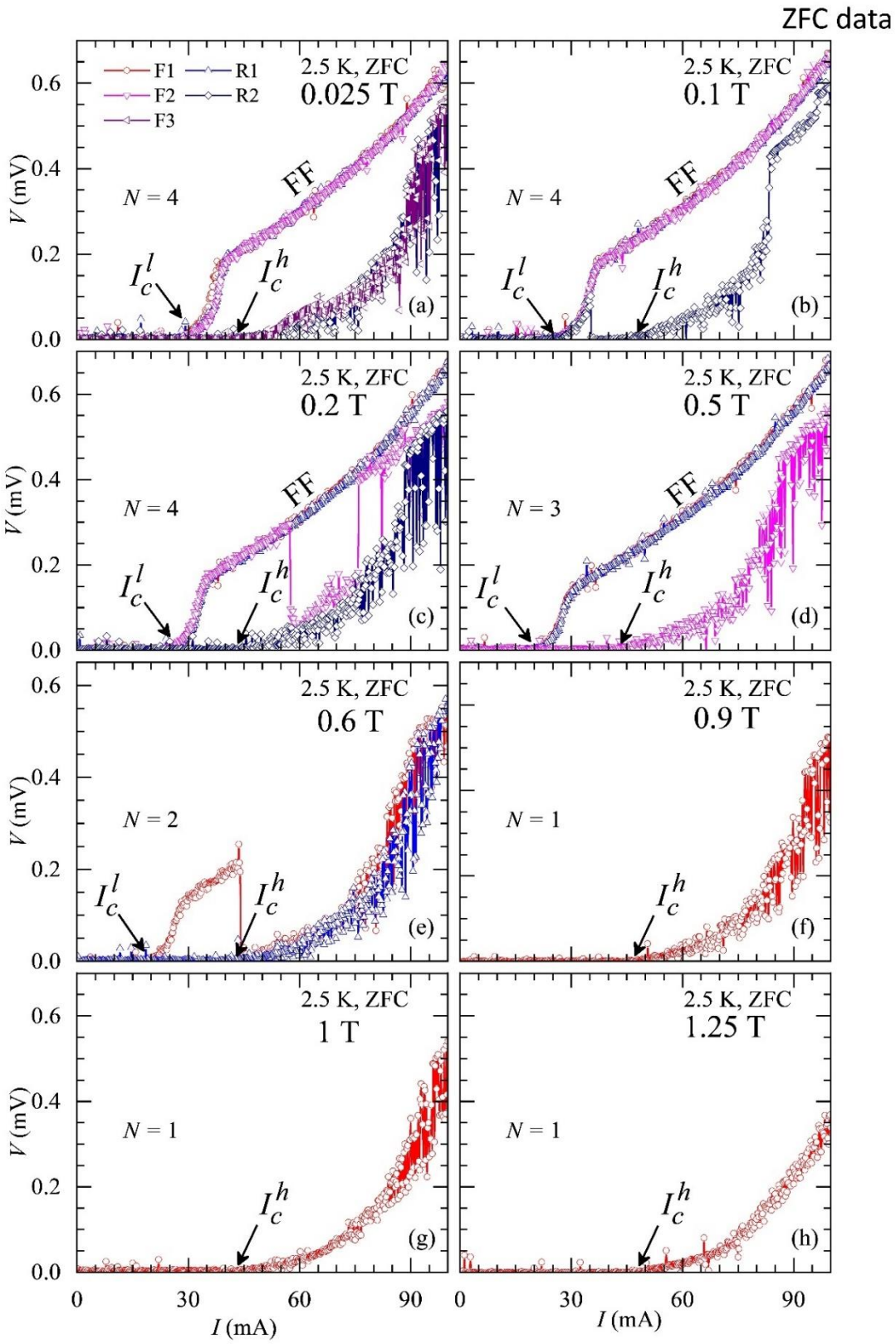

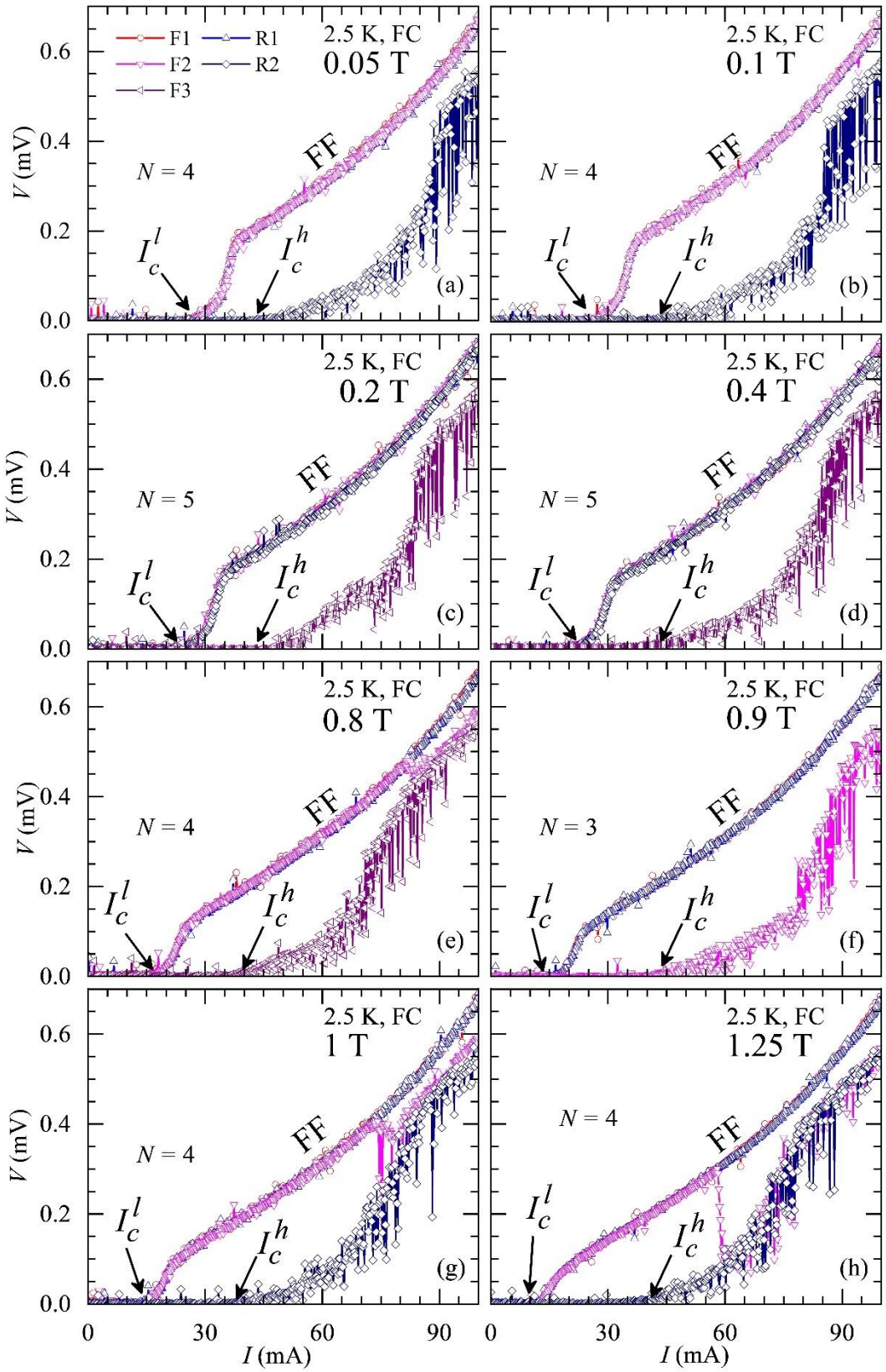
F1
F2
F3
R1
R2
2.5 K, FC
0.05 T
0.1 T
0.2 T
0.4 T
0.8 T
0.9 T
1 T
1.25 T
N = 4
N = 5
N = 3
FF
I_c^l
I_c^h
(a)
(b)
(c)
(d)
(e)
(f)
(g)
(h)
V (mV)
I (mA)
0.0
0.2
0.4
0.6
0
30
60
90

FC data

6. **Nine *I-V* cyclings. After 4 cycles (F1, R1, F2, R2), the high I_c^hstate is reached (in F3). After that further cycles F3, R3, F4, R4, F5 keeps the system in the high I_c^hstate.**

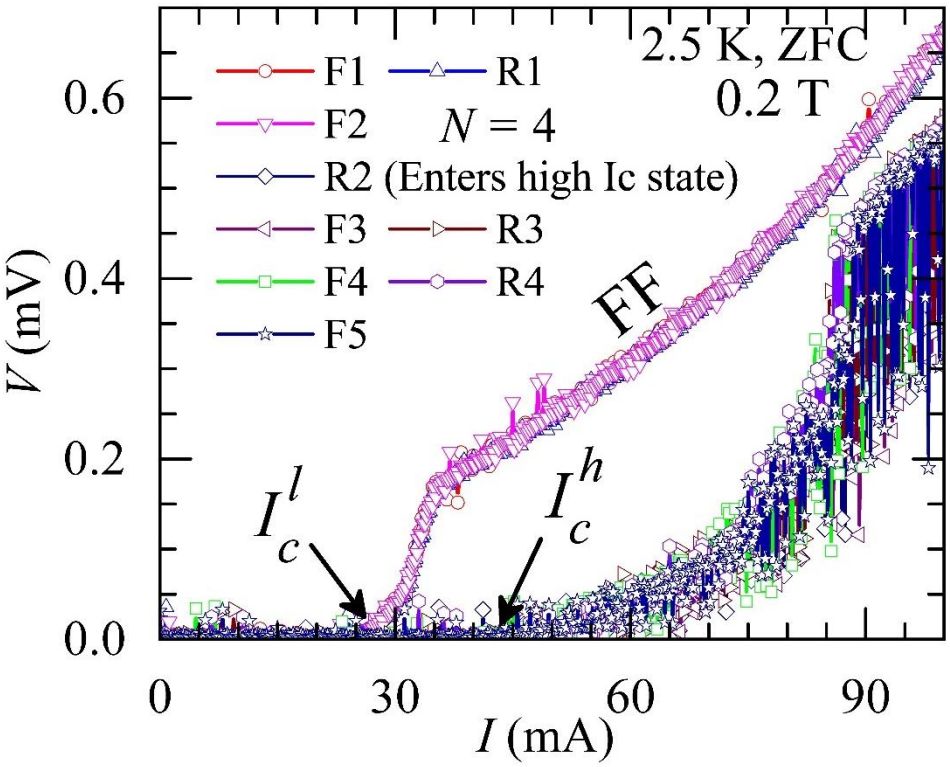

7. Temperature very near the sample during *I-V* measurement.

Temperatures as measured by the temperature sensor At 2.5 K, when the current(I) is ramped up to 100 mA.

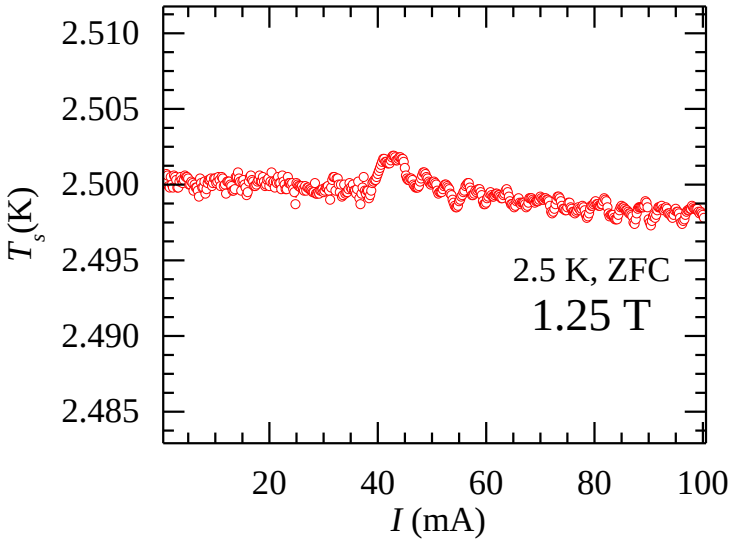

Figure S5: Variation of sample temperature while increasing *I* during *I-V* measurement at 2.5 K and 1.25 T

We show a measurement of sample temperature (T_s) as recorded by the temperature sensor located ~ 1.0 mm away from the sample, at 2.5 K. This $T_s(I)$ measurement is performed, during the *I-V* measurement as current is increased upto 100 mA. Note that that most of the fluctuations in T_s are well within 5 mK during the *I-V* measurements.

8. Variation of dissipation with drive

In figure S6, we have replotted the *I-V* data in Figs. 1(a),(b) in terms of normalized resistivity $\left(\rho/\rho_f,\right.$ where ρ:resistivity and ρ_f: Bardeen-Stephen flux flow resistivity$\left.\right)$ as a function of I where $\rho_f = \rho_n \frac{B}{B_{c2}}$, $\rho_n = 60$ μΩ-cm (normal state resistivity) and higher critical magnetic field, B_{c2} = 2.5 T (at 2.5 K). It shows that for the F1, R1 and F2 (for details see the manuscript) after depinning from the pristine vortex state at I_c^l ~ 23 mA, we observe sharp enhancement in dissipation (ρ) with drive (I) in the thermally activated flux flow regime (TAFF) and the driven vortex state transforms into the flux flow (FF) state beyond I_{cr}. The most noteworthy feature in Fig. S6 is that the dissipation is almost constant (ρ/ρ_f ~ 7) in the FF regime for F1, R1 and F2 runs. Additionally, in the FF regime the driven vortex matter for the F2 run exhibits NDR transition (at I ~ 45 mA, for details see the main text) and falls to a drive-induced immobile state (high I_c state) which depins at I_c^h, following a noisy response in *IV* or $\rho/\rho_f(I)$. However, the dissipation levels in this fluctuating levels are considerably small compared to the FF state. This fluctuating dissipation response turns uniform and merges with the FF state beyond I ~ 80 mA.

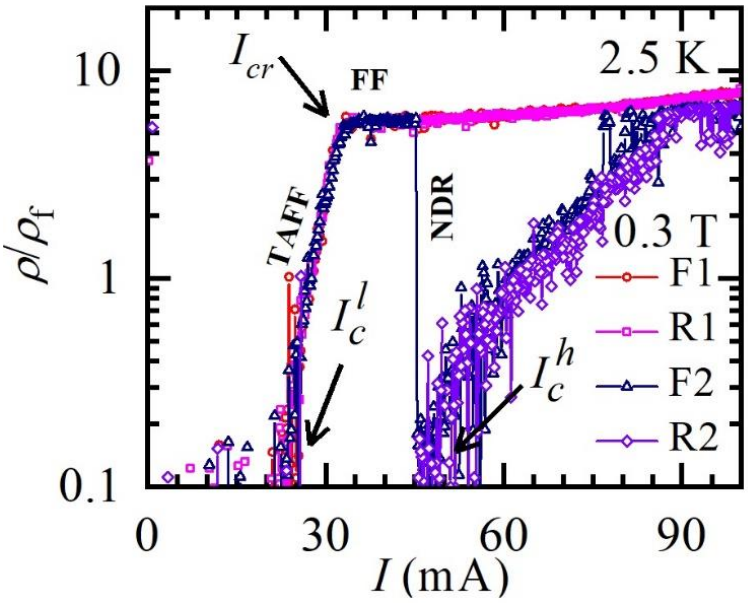

Figure S6: ρ/ρ_f vs I (in log linear scale) at 2.5 K and 0.3 T for F1, R1, F2 and R2 runs.